

# EFFECTS OF pH ON AGGLOMERATION STATE OF $\text{Al}_2\text{O}_3 - \text{ZrO}_2$ (ZTA) NANOCOMPOSITE POWDERS SYNTHESIZED BY TARTARIC GEL METHOD

#MUSTAFA TUNCER, #HASAN GOCMEZ

*Department of Ceramic Engineering, Dumlupınar University, Kutahya, Turkey*

#E-mail: hasangocmez@yahoo.com

Submitted July 20, 2011; accepted March 28, 2012

**Keywords:** Composite material, Sol-gel, Agglomeration, pH

*Alumina – 20 vol% zirconia (ZTA) nanocomposites were synthesized by the tartaric acid sol-gel method. The precursors gelled from solutions at different pH were prepared and then calcined from 1000 to 1500°C. Surface area measurement (BET), X-ray diffraction (XRD), scanning electron microscopy (SEM) and transmission electron microscopy (TEM) were used to characterize the synthesized powders. Control of agglomeration state was carried out by changing the pH of the solution. Weakly agglomerated powders were obtained at pH=6, whereas the solution at pH=1 revealed hard agglomerated powders, (agglomeration degrees, N, were found to be 16425 at pH=1 and 102 at pH=6, respectively). The pH dependence of agglomeration was explained by the dissociation behavior of tartaric acid at various pH environments. XRD results showed that the powders have been fully tetragonal phase at 1000°C, while they exhibited tetragonal zirconia with minor monoclinic phase as well as  $\alpha\text{-Al}_2\text{O}_3$  at 1500°C. The presence of  $\alpha\text{-Al}_2\text{O}_3$  in the nanocrystalline composite contributes the wide range of temperature stability for  $t\text{-ZrO}_2$  up to 1500°C. TEM micrograph confirmed that alumina and zirconia were dispersed homogeneously. Mechanical properties (hardness and indentation fracture toughness) of sintered samples were also determined.*

## INTRODUCTION

There have been intense researches on the preparation of nanocomposite ceramics to improve the engineering properties of monolithic ceramics [1,2]. Zirconia toughened alumina (ZTA) is the one of these composites, which have emerged in structural applications because of its superior properties such as excellent strength, toughness, thermal shock resistance, wear resistance and chemical stability. ZTA composites have been widely used in the application of biomaterial, structural materials (high-temperature gas burner, industry structures, cutting tools, and bearing balls) and catalytic support [3-6].

Several techniques for synthesizing alumina-zirconia powders have been reported in literature such as colloidal processing [7], solution combustion [8] coprecipitation [9], chemical vapor deposition [10], sol-gel synthesis [11], mechanical mixing [12] and so on. The gel method is a wet chemical technique and very effective way for preparing homogenous composite powder with high purity. It represents a much faster and easier process at relatively lower temperatures. It also enables molecular level mixing, which leads to homogeneous and well dispersed microstructures [13]. This method is based on the formation and calcination of polymeric networks of metal-organic precursors. Organic acids such as citrate,

tartaric and glycolic acid, having the ability of forming complexes with ions, are used as gelation agents that have functional groups reacting with metal ions (chelate) to form a gel. Homogenous solutions consisting of metal ions and organic acid in water are prepared. The three-dimensional polymeric networks ions are formed by ion chelation with the functional group of acid. As a result of this, the solution turns into a highly viscous condition with increasing temperature and then a gel is formed. Finally, the gel is decomposed at moderate temperature to obtain ceramic powder [14, 15].

The properties and performance of the final material depend on the characteristics of the starting powders, synthesis conditions and processing steps (mixing, calcination, drying). An important issue in powder processing is the agglomeration during the synthesis. The primary particles get together to form large and inhomogeneous structures with porosity (agglomerates). Agglomeration leads to inhomogeneous packing during compaction and defects in the green/sintered compacts, and inhomogeneous microstructure, deteriorating the engineering properties of materials. Therefore, it is essential to prevent powders against agglomeration. As nano-size powder processing is considered in nanotechnology, it is required to synthesize agglomerate-free (or weakly agglomerated) powders [16-19].

In the present study, the production of ZTA ( $\text{Al}_2\text{O}_3 - 20 \text{ vol } \% \text{ ZrO}_2$ ) composite nanopowder with agglomeration controlled via pH during synthesis was investigated. The hardness and toughness of fabricated composite powders were examined as well.

## EXPERIMENTAL

$\text{ZrOCl}_2 \cdot 8\text{H}_2\text{O}$  (Fluka, 99 %),  $\text{Al}(\text{NO}_3)_3 \cdot 9\text{H}_2\text{O}$  (Sigma, 98 %) and  $\text{YCl}_3$  (Fluka, 99 %) were used as starting materials. Tartaric acid (Fluka, 99.5%) and distilled water were used as gelation agent and solvent, respectively. The pH of the solution was adjusted with  $\text{NH}_4\text{OH}$ . The gelation experiment was carried out by firstly dissolving tartaric acid into  $100 \text{ cm}^3$  of water in a beaker, and then the required amount of aluminum nitrate, zirconium oxychloride and yttrium chloride were added into the tartaric acid solution according to the final composition containing 20 vol% zirconia (doped with 2 mol% yttria). The solution was continuously stirred at room temperature until a highly transparent solution was obtained. The pH of the solution measured after getting a clear aqueous solution was close to 1, solutions having different pH (3, 6 and 9) were prepared by adding ammonium. The temperature was kept at  $80^\circ\text{C}$  for 60 min while and then heated to  $200^\circ\text{C}$  to initiate the gelation reaction. As the water evaporated, the viscosity of the precursor solution increased and finally turned into a yellowish sticky gel. The gel was conveyed to a mantle heater at  $400^\circ\text{C}$  for 8 h to remove organic matter in air. Finally, the obtained "ceramic gel precursor" was crushed gently in an agate mortar and then dried at  $90^\circ\text{C}$  overnight. Heat treatment for gel precursors was carried out at  $1000^\circ\text{C}$  and  $1500^\circ\text{C}$  for 2 h. The composite ceramic nanopowders were ground and sieved with 90 micron size screen. The crystallization and structural development of ZTA was studied by X-ray diffractometry (Rigaku, Miniflex) using  $\text{Cu K}_\alpha$  radiation. The crystallite size  $d_{\text{XRD}}$  was calculated from the Scherrer formula from the XRD broadening. The microstructure of the calcined powders and sintered products polished by diamond paste and thermally etched at  $1250^\circ\text{C}$  for 5 h were observed by field emission scanning electron microscopy (Zeiss Supra 50 VP). Samples were then gold coated for scanning electron microscope (SEM) analysis. Transmission electron microscopy (TEM, Jeol JEM-2010F) operated at 200 kV was used to obtain the nanocrystal images. The specimens were prepared by slow evaporation of a drop of the sample suspension deposited onto a copper grid with a carbon film. The surface area of the powders was measured via the  $\text{N}_2$  adsorption isotherm at  $-196^\circ\text{C}$  using the BET equation on a Quantachrome Nova 2200 E instrument. Prior to the  $\text{N}_2$  adsorption, the powders were degassed at  $200^\circ\text{C}$  for 2 h under vacuum. The average particle size was calculated by the following equation from the surface area data, which is called  $d_{\text{BET}}$ .

$$d_{\text{BET}} = \frac{6}{S \cdot \rho} \quad (1)$$

( $\rho$  = density,  $\text{g}/\text{cm}^3$  and  $S$  = surface area,  $\text{m}^2/\text{g}$ )

The density of the powders was determined using by a helium gas pycnometer (Quantachrome Ultrapyc 1200e). The degree of agglomeration was calculated as follows:

$$N = \frac{d_{\text{BET}}^3}{d_{\text{XRD}}^3} \quad (2)$$

( $N$  = the degree of agglomeration,  $d_{\text{BET}}$  = the average particle size from surface area,  $d_{\text{XRD}}$  = the average crystallite size from XRD peak broadening) [20]. The powder was granulated (a few drops of 2 % PVA solution was added as a binder) and pressed as green compacts to evaluate their sintering behavior. Green compacts were sintered at  $1500$  and  $1600^\circ\text{C}$  for 5 h. The relative densities of the sintered ceramics were measured using Archimedes' method. Vickers hardness was measured using a static microhardness tester (Future-Tech). Before hardness measurements, the samples were molded with epoxy resin and surface damage was removed mechanically by grinding with 2400 and 4000 grit, and then polishing on 6, 3 and 1 mm diamond lap wheels. Hardness measurement was made at 9.8 N load with a loading time of 15 s. The indentation diagonal lengths were measured with a Nikon MA 100 inverted metal microscope using the Clemex Professional microscopy image analysis software.  $50\times$  and  $20\times$  objective lenses were used on the Nikon MA 100 instrument. In view of the scatter of the microhardness data, the hardness value was a mean of at least six measurements under the same condition. The hardness values ( $H_V$ ) from the length of the two diagonals of the squareshaped Vickers indents were calculated with the equation:

$$H_V = 1.854(F/D^2) \quad (3)$$

where  $F$  is the applied force (in Newton) and  $d$  the diagonal length (in mm) of the indentation. The value of the hardness at 9.8 N and extended corner cracking was used to calculate the fracture toughness ( $K_{\text{IC}}$ ) with the Evans [21] and Anstis et al. [22] methods. A value of 350 GPa, which is the elastic modulus of ZTA ( $\text{Al}_2\text{O}_3 - 20 \text{ vol } \% \text{ ZrO}_2$ ), was used in the calculation of indentation fracture toughness.

## RESULTS AND DISCUSSION

XRD pattern of powders gelled at different pH and subsequently calcined at  $1000^\circ\text{C}$  for 2 h are shown in Figure 1. At all pH values, the tetragonal zirconia with small diffraction peaks of  $\alpha$  and other phases of alumina were examined. The crystallite size of  $\alpha$ -alumina changed between 9 and 12 nm.

After sintering at  $1500^\circ\text{C}$ , a mixture of tetragonal zirconia with minor monoclinic zirconia and  $\alpha$ -alumina was detected in all powders (Figure 2). The crystallite size

of  $\alpha$ -alumina varied from 46 to 52 nm. The XRD results of samples prepared at any pH showed that zirconia was successfully stabilized over a wide temperature range. It is known that the stabilization of tetragonal phase at room temperature is one of the mechanisms to improve mechanical properties of composites. In this study, zirconia particles were dispersed into the alumina matrix, which hindered the transformation of tetragonal to monoclinic phase in a wide temperature range.

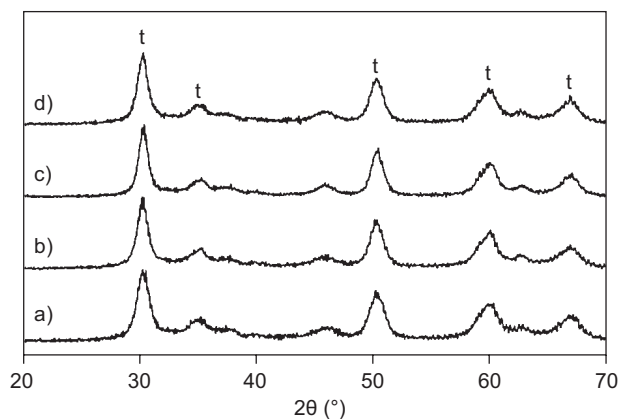


Figure 1. The XRD pattern of composite powders calcined at 1000°C for 2 h after synthesized from solutions at: a) pH 1, b) pH 3, c) pH 6, d) pH 9 (t - tetragonal zirconia).

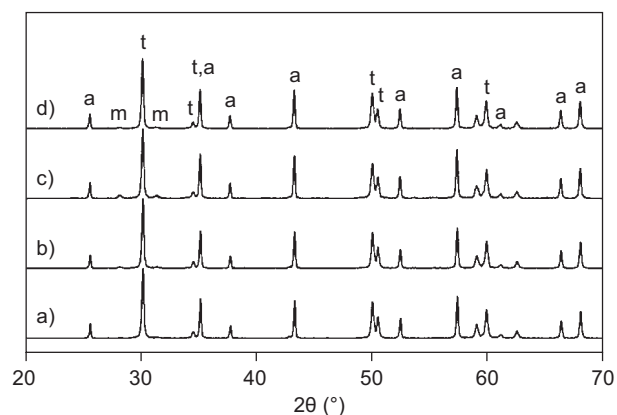


Figure 2. The XRD pattern of composite powders calcined at 1500°C for 2 h after synthesized from solutions at: a) pH 1, b) pH 3, c) pH 6, d) pH 9 (t - tetragonal zirconia, a - corundum type alumina, m - monoclinic zirconia).

Table 1 presents the results of surface area, density, particle size and crystallite size for Al<sub>2</sub>O<sub>3</sub>-ZrO<sub>2</sub> nanocomposites calcined at 1000°C for 2 h. The surface area and particle size were 7.5 m<sup>2</sup>/g and 233.9 nm for pH=1, whilst these values were 34.9 m<sup>2</sup>/g and 54.1 nm for pH=6, respectively. The surface area from BET and line broadening from XRD were used in calculation of particle size and crystalline size, respectively. In the BET technique, the surface of a volume filled with a solid is calculated, while XRD line broadening determines the coherently diffracting domain size. The different size values obtained from these two techniques can be used for calculating the agglomeration state of the powders. The number of crystallites (grains) per particle is a simple measure for the degree ( $N$ ) of agglomeration. As this value becomes smaller or ( $N$  value close to unity), particles tend to approach their primary size, which may be classified as loose or weakly agglomerated powders [20]. At pH=6, a less agglomerated powder was obtained ( $N=102$ ), whereas at pH=1 (natural pH for solution) a strongly agglomerated powder ( $N=16425$ ) was synthesized. The  $N$  value of ZAl1 powders is 160 times higher than that of ZAl6. The results revealed that the changing pH of solution had an ultimate effect on modification of agglomeration. Consequently, the properties of powders are modified by altering the pH value.

It is believed that the possible mechanism on dependence of agglomeration to pH may be due to dissociation behavior of tartaric acid at various pH values. For pH=1, the tartaric acid has weak dissociation leading to closer interaction between a cation and functional groups of the acid. Upon heat treatment, the oxide particles might come together to give rise to agglomeration. The distance between cations and functional groups in the backbone of tartaric acid is higher because of the high dissociation of tartaric acid at pH=6. This result in less contact between the particles during the heat treatment.

A SEM image of as-received powder (ZAl6) obtained after mantle heater treatment is shown in Figure 3. The powders have a flake morphology and a broad size distribution. The porous structure of the powder results in removal of gas species during combustion reactions.

Strongly agglomerated powders were obtained at pH=1 (Figure 4a), but the synthesis at pH=6 produced less agglomerated powder with a high surface area

Table 1. The characteristics of Al<sub>2</sub>O<sub>3</sub> - 20 vol% ZrO<sub>2</sub> composite powders calcined at 1000°C for 2 h (S.A: surface area,  $d_{\text{BET}}$ : particle size of Al<sub>2</sub>O<sub>3</sub> from BET,  $d_{\text{XRD}}$ : crystalline size of Al<sub>2</sub>O<sub>3</sub> from XRD,  $N$ : degree of agglomeration).

Powders	pH of Solution	S.A.at 1000 °C (m <sup>2</sup> /g)	$d_{\text{BET}}$ (nm)	$d_{\text{XRD}}$ (nm)	Density (g/cc)	$N$ ( $d_{\text{BET}}^3/d_{\text{XRD}}^3$ )
ZAl1	1	7.5	233.9	9.2	3.43	16425
ZAl3	3	9.8	164.8	11.3	3.72	3100
ZAl6	6	34.9	54.1	11.6	3.18	102
ZAl9	9	18.5	99.3	10.6	3.27	822

(Figure 4b). The size values calculated from BET and XRD are close to each other for ZA16, indicating that intraparticle pores remain accessible in agglomerates and

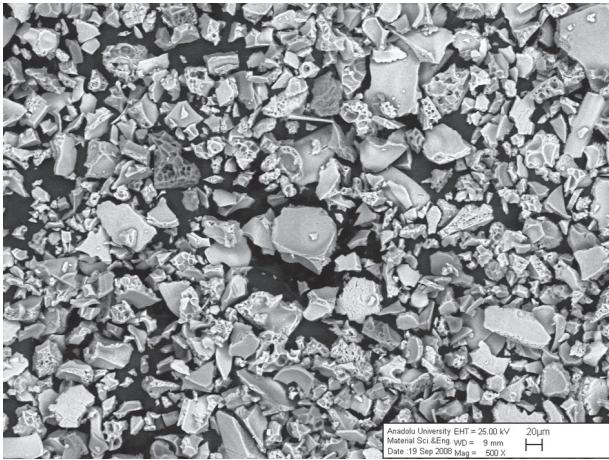
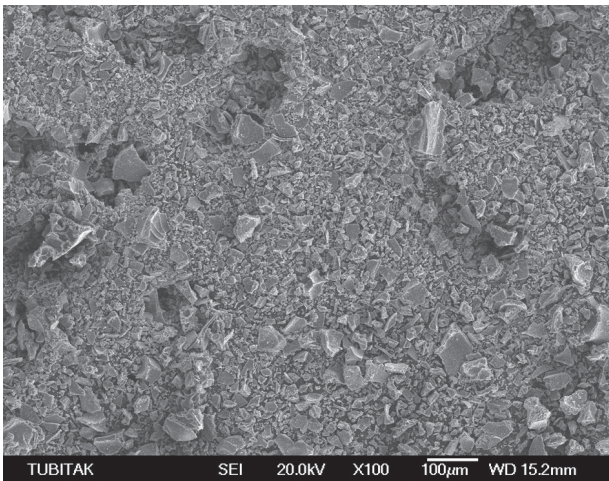
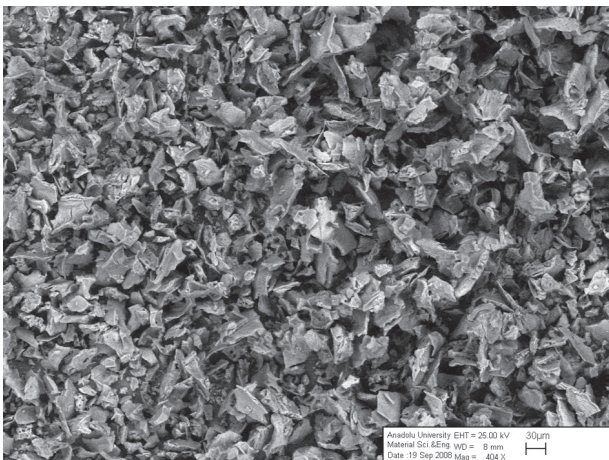


Figure 3. SEM images of as-synthesized ZA16 gel after burning in a mantle heater.



a)



b)

Figure 4. SEM images of powders (1000°C for 2 h) gelled from solution of: a) pH 1, b) pH 6.

the nitrogen gas can diffuse the particle spaces. Thus, powders contacted weakly each other, which represents soft agglomeration.

The TEM micrograph (Figure 5) of ZA16 calcined at 1000°C exhibited a very homogeneous nanostructure with an equiaxed-rounded shape of particles. The dark regions on the image represent zirconia particles and the bright ones indicate alumina particles. In addition, the crystallite size was in good agreement with XRD results.

It is important to obtain homogeneously dispersed particles for better microstructure which lead to the desired properties of final materials [23]. Therefore, the powder with lower  $N$  value (AZ16) was selected to evaluate the sintering process. The density and sintering temperature of the compacts are shown in Table 2. The obtained densities were over 99 % of theoretical ones. In Figure 6, homogeneously dispersed zirconia grains (bright phase) in an alumina matrix (dark phase) were obtained, which presents the advantage of gel synthesis in producing nanocomposites.

Table 2. The densities of ZA16 compact at different sintering temperatures.

Samples	Sintering Temperature (°C)	R.D. (%)
ZA116-1500	1500	99.6
ZA116-1600	1600	99.7

Table 3 shows the Vickers hardness ( $H_v$ ) and indentation fracture toughness ( $K_{IC}$ ) values of sintered composites compacted from ZA16 powder at 1600 °C for 5 h. The hardness value of the dense material was measured to be 7.9 GPa under 9.8 N load. The indentation fracture toughness calculated using the Anstis and Evans equations were 3.2 and 2.9 MPam<sup>1/2</sup>, respectively. It must be emphasized that different values of mechanical properties can be obtained depending on differences in processing techniques, powder characteristics and measurement techniques (e.g. hardness).

Table 3. The hardness and indentation fracture toughness values of ZA16 compact sintered 1600°C for 5 h.

Sample	Hardness under the 9.8 N load (GPa)	$K_{IC}$ , Anstis (MPam <sup>1/2</sup> )	$K_{IC}$ , Evans (MPam <sup>1/2</sup> )
ZA16-1600	7.9	3.2	2.9

## CONCLUSION

Nanocomposite powders were successfully synthesized by a sol-gel based method. The results show that the agglomeration state of the powders can be easily controlled by changing pH during synthesis. Weakly (soft) agglomerated ZTA nanopowders were obtained from solution at pH=6, in which the  $N$  factor was found

to be lower. The pH dependence of agglomeration was related to the dissociation of organic acid. The tetragonal zirconia with minor monoclinic phase remained stabilized in a wide temperature range from room temperature to 1500°C. Alumina grains matrix hindered tetragonal-monoclinic phase transformation of zirconia. The improvement in mechanical properties is essentially related to homogeneously dispersed particles in the microstructure. Consequently, the gel method allows powders to be synthesized with a tailored agglomeration state, as well as tailored physical properties, by changing the pH of the solution.

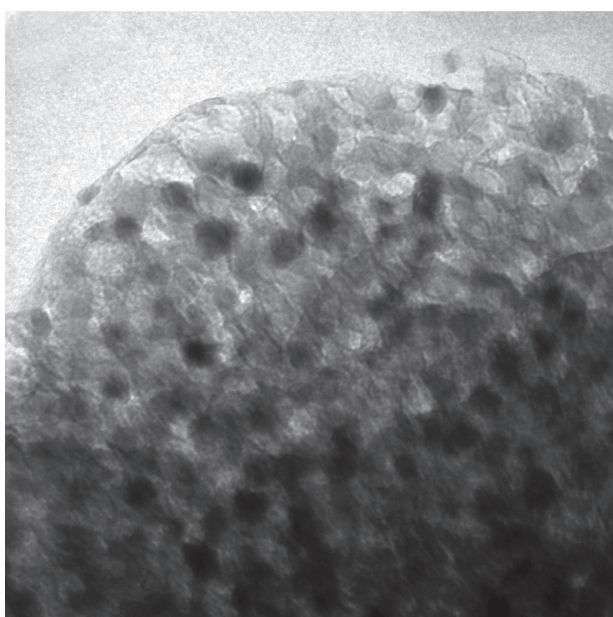


Figure 5. TEM image of ZTA16 powders calcined at 1000°C for 2 h.

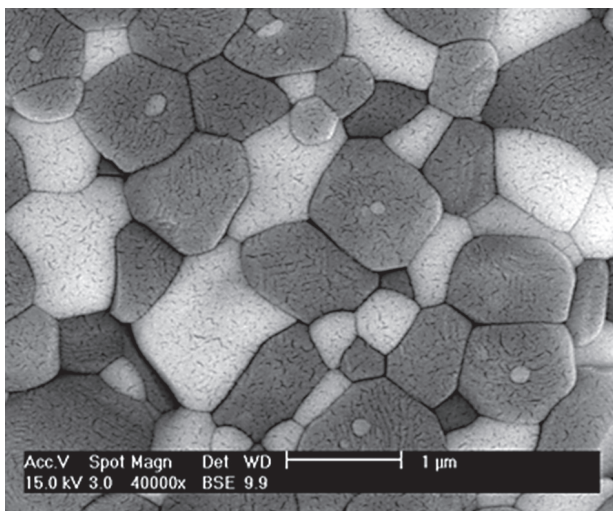


Figure 6. SEM images of the thermally etched surface of composite compacted from ZTA16 powder.

#### Acknowledgements

The financial supports provided by the Scientific and Technological Research Council of Turkey (TUBITAK, project no: 107M367) are gratefully acknowledged.

#### References

1. Yoshimura M., Tag Oha S., Sandob M., Niihara K.: *J. Alloys and Comp.* 290, 284 (1999).
2. Kong Y. M., Kim H. E., Kim H. W.: *J. Am. Ceram. Soc.* 90, 298 (2007)
3. Weimin M., Lei W., Renguo G., Xudong S., Xikun L.: *Mater. Sci. and Eng. A.* 477, 100 (2008).
4. Enache D., Auberger M. R., Esterle K., Revel R.: *Physicochem. Eng. Aspects.* 220, 223 (2003).
5. Bartolomé J. F., De Aza A. H., Martín A., Pastor J. Y., Llorca J., Torrecillas R., Bruno G.: *J. Am. Ceram. Soc.* 90, 3177 (2007).
6. Kong Y. M., Kim H. E., Kim H. W.: *J. Am. Ceram. Soc.* 90, 298 (2007).
7. Aksay I. A., Lange F. F., Davis B. I.: *J. Am. Ceram. Soc.* 66, 190 (1983).
8. Chandradass J., Kim K. H.: *Met. Mater. Int.* 15, 1039 (2009).
9. Murase Y., Kato E., Daimon K.: *J. Am. Ceram. Soc.* 69, 83 (1986).
10. Hori S., Yoshimura M., Somiya S., Takahashi R.:  $Al_2O_3$ - $ZrO_2$  ceramics prepared from CVD powders, in: N. Claussen, M. Ruhle, A.H. Heuer (Eds.), *Advances in Ceramics*, vol. 12, p. 794–80, Science and Technology of Zirconia II, The American Ceramic Society, Columbus, Ohio, 1984.
11. Saha A., Agrawal D. C.: *J. Mater. Sci. Let.* 17, 1333 (1998).
12. Murase Y., Kato E., Daimon K.: *J. Am. Ceram. Soc.* 69, 83 (1986).
13. Hon Y. M., Lin S. P., Fung K. Z., Hon M. H.: *J. Eur. Ceram. Soc.* 22, 653 (2002).
14. Hongtem T., Kaowphong S., Thongtem S.: *Ceram. Int.* 33, 1449 (2007).
15. Gocmez H., Fujimori H., Tuncer M., Gokyer Z., Duran C.: *Mater. Sci. and Eng. B.* 173, 80 (2010).
16. Deng Z. Y., Zhou Y., Inagaki Y., Ando M., Ohji T.: *Acta Mater.* 51, 731 (2002).
17. Shin H. S., Lee B. K.: *J. Mater. Sci.* 32, 4803 (1997).
18. Shi J. L., Gao J. H., Lin Z. X., Yan D. S.: *J. Mater. Sci.* 32, 4803 (1997).
19. Balakrishna P., Murty B. N., Anudradha M.: *J. Nuclear Mater.* 384, 190 (2009).
20. Winterer M.: *Nanocrystalline Ceramics - Synthesis and Structure*, Springer Series in Materials Science, Vol. 53, Springer Verlag, New York, 2002.
21. Evans G.: *Fracture toughness: The role of indentation techniques*, edited by S.W. Freiman, *Fracture mechanics applied to brittle materials ASTM STP 678 American Society for Testing and Materials*, p.112, Blacksburg 1979.
22. Anstis G. R., Chantikul P., Lawn B. R., Marshall D. B.: *J. Am. Ceram. Soc.* 64, 533 (1981).
23. Lange F. F.: *J. Am. Cer. Soc.* 67, 83 (1984).